

GOES-R Risk Reduction Semi-Annual Report:

PIs: Sanmei Li and Donglian Sun

Reporting Period: 01/01/2018-06/30/2018

Project Title: Integration of GOES-R/ABI data in Flood Mapping Software for Flood Monitoring and Forecasting

Executive Summary

Overall Status: Green

	Green ¹ (Controlled)	Yellow ² (Caution)	Red ³ (Critical)	Deviation Summary ⁴
Budget	<input checked="" type="checkbox"/>	<input type="checkbox"/>	<input type="checkbox"/>	
Schedule	<input checked="" type="checkbox"/>	<input type="checkbox"/>	<input type="checkbox"/>	
Scope	<input checked="" type="checkbox"/>	<input type="checkbox"/>	<input type="checkbox"/>	

¹Project is within budget, scope and on schedule.

²Project has deviated slightly from the plan but should recover

³Project has fallen significantly behind schedule, is forecast to be significantly over budget, and/or has taken on tasks that are out of scope.

⁴Details of deviations provided in subsequent section of report

Comments:

Scheduled Milestones/ Deliverables

Milestone	Approved Schedule	Start Date	Forecasted Completion	Actual Completion	Status
Milestone Title					
Algorithm adjustment and improvement based on the existing VIIRS algorithms	July 2017	Jan. 01, 2018	April. 30, 2018	June 30, 2018	Completed
Algorithm integration to flood mapping software, algorithm and software performance test, evaluation and improvements	July 2017	May 01, 2018	Oct. 31, 2018	Dec. 31, 2017	In progress
Website framework design	July 2017	Dec. 01, 2017	April 30, 2018		In progress

Note: Bold milestones are key external project deliverables

Status Definition: Green (will meet schedule), Yellow (milestone will be delayed), Red (milestone cannot be met on current path)

Accomplishments during this Reporting Period:

1. GOES-16/ABI data correction

1.1. Issues with the ABI reflectance channels

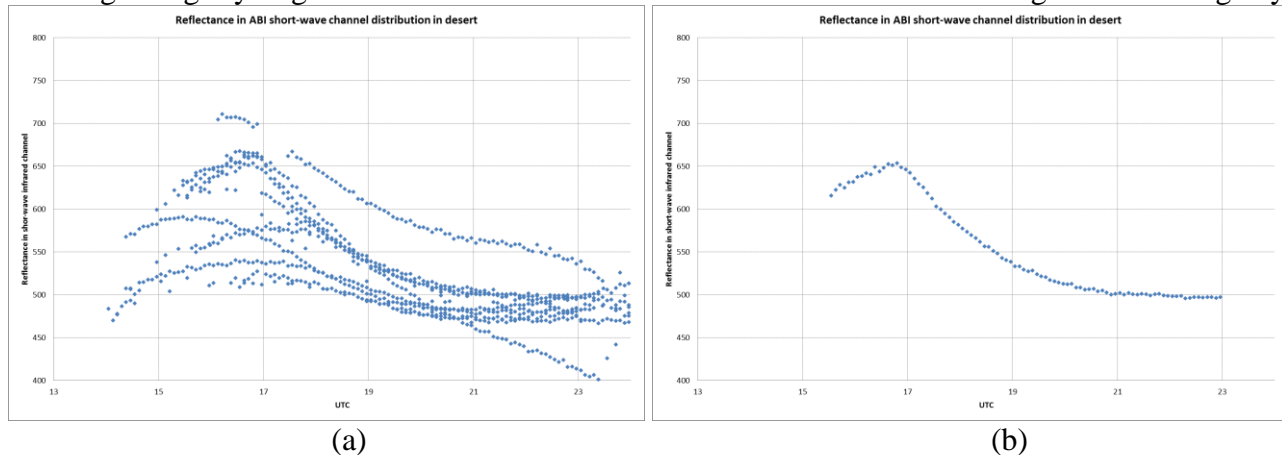
With the work we did in 2017, the framework of the ABI flood mapping software has been completed and the software can be used for ABI flood mapping automatically. Later, the software has been tested with the ABI imagery year around. Overall, the test results in summer seasons are quite steady. However, in winter seasons, some issues were found. These issues can be summarized in three aspects:

- 1) The reflectance of ABI visible, near-infrared and short-wave infrared channels shows some diurnal change, and the fluctuation of reflectance may vary about 25% to 30%.
- 2) The diurnal change patterns vary with land cover types and seasons.
- 3) The reflectance of the short-wave infrared channel is a little bit higher than other satellite imagery such as VIIRS.

While the reflectance of the three channels (visible, near infrared and short-wave infrared) show similar diurnal change patterns, only the analyses on the reflectance in the ABI short-wave infrared channel is presented in this document. Fig.1 and Fig. 2 demonstrate some figures of the diurnal reflectance distribution in the ABI short-wave infrared channel. The samples in Fig. 1 were all collected from the same region around (114.7° W, 32.22°N), where the land cover is mostly desert; while the samples in Fig. 2 were collected from different locations, in which one scatter series is from the same ABI pixel over vegetation, non-sand bare land or water surface.

From Fig. 1, the reflectance is much higher in the morning than that in the afternoon, and reaches the peak between 16:00 and 17:00 UTC. The reflectance in the morning can vary 25% to 30%; while in the afternoon, the reflectance is more consistent. The reflectance also shows some seasonal patterns: the fluctuation is larger in winter seasons than in summer seasons.

Different from desert, vegetation and non-desert bare land show a diurnal change pattern: reflectance increases from the morning to the noon and then decreases from the noon to the afternoon, which is consistent to the diurnal change pattern of solar zenith angles (Fig. 2). The fluctuation in the morning is slightly larger than in the afternoon. Pure water surface doesn't change much during daytime.



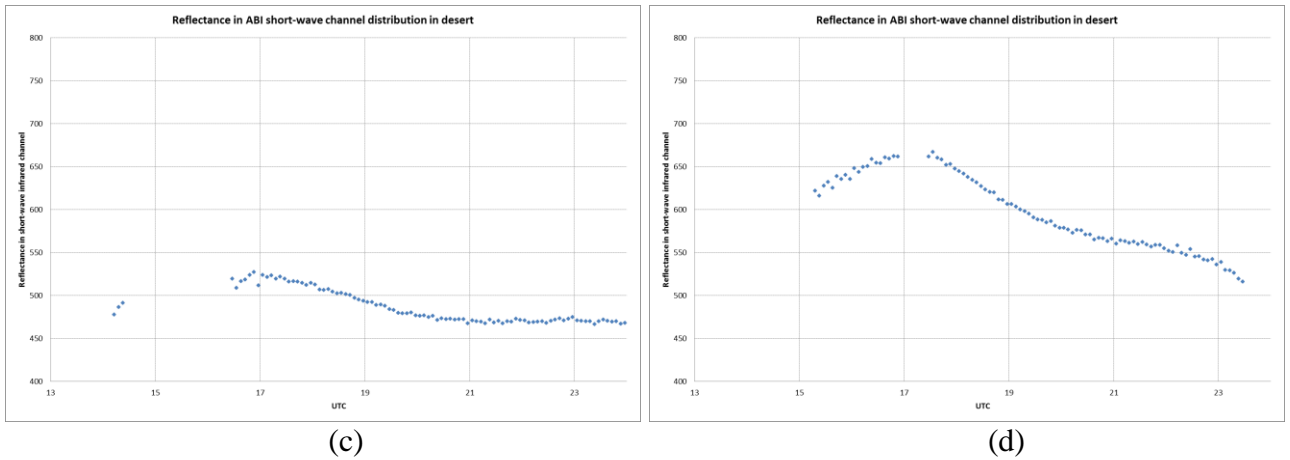


Fig. 1 Reflectance of the ABI short-wave infrared channel in desert: (a) samples collected year around; (b) Samples on Feb. 25, 2018; (c) Samples on May 02, 2017; (d) Samples on Oct. 29, 2017

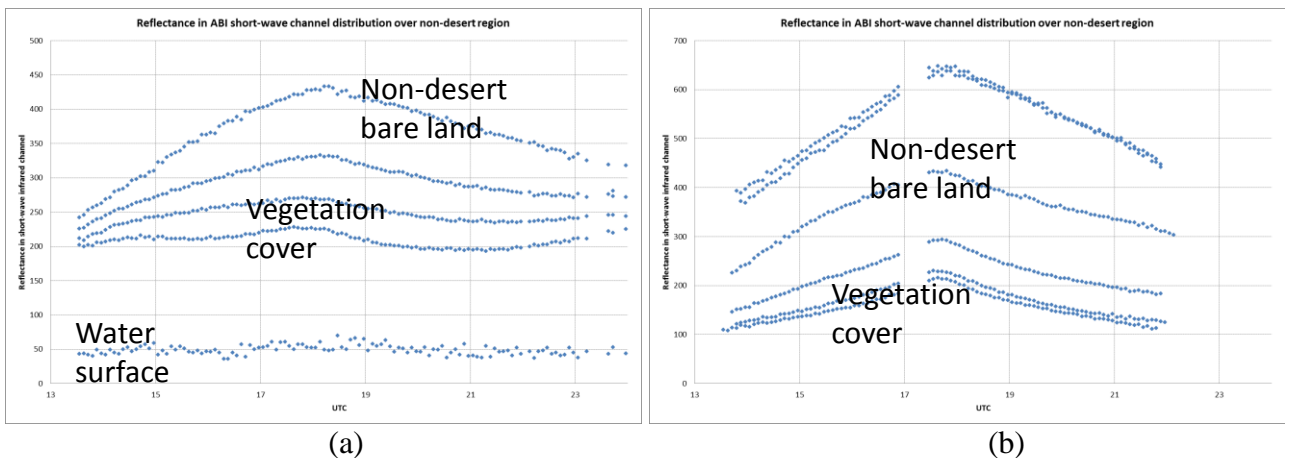


Fig. 2 Reflectance of the ABI short-wave infrared channel in vegetation, water surface and non-desert bare land: (a) samples on Aug. 17, 2017; (b) Samples on Oct. 29, 2017

These diurnal change patterns in the ABI reflectance channels cause uncertainty to the flood detection when we adjust the VIIRS flood algorithms to the ABI imagery. Fig.3 shows an example of an ABI false-color composited image and the corresponding flood map on Jan. 01, 2018 at 16:48 (UTC). From Fig. 3, the detection results misclassify many clear-sky pixels (snow cover, bare land and so on) as cloud cover, and many mixed water pixels are not identified.

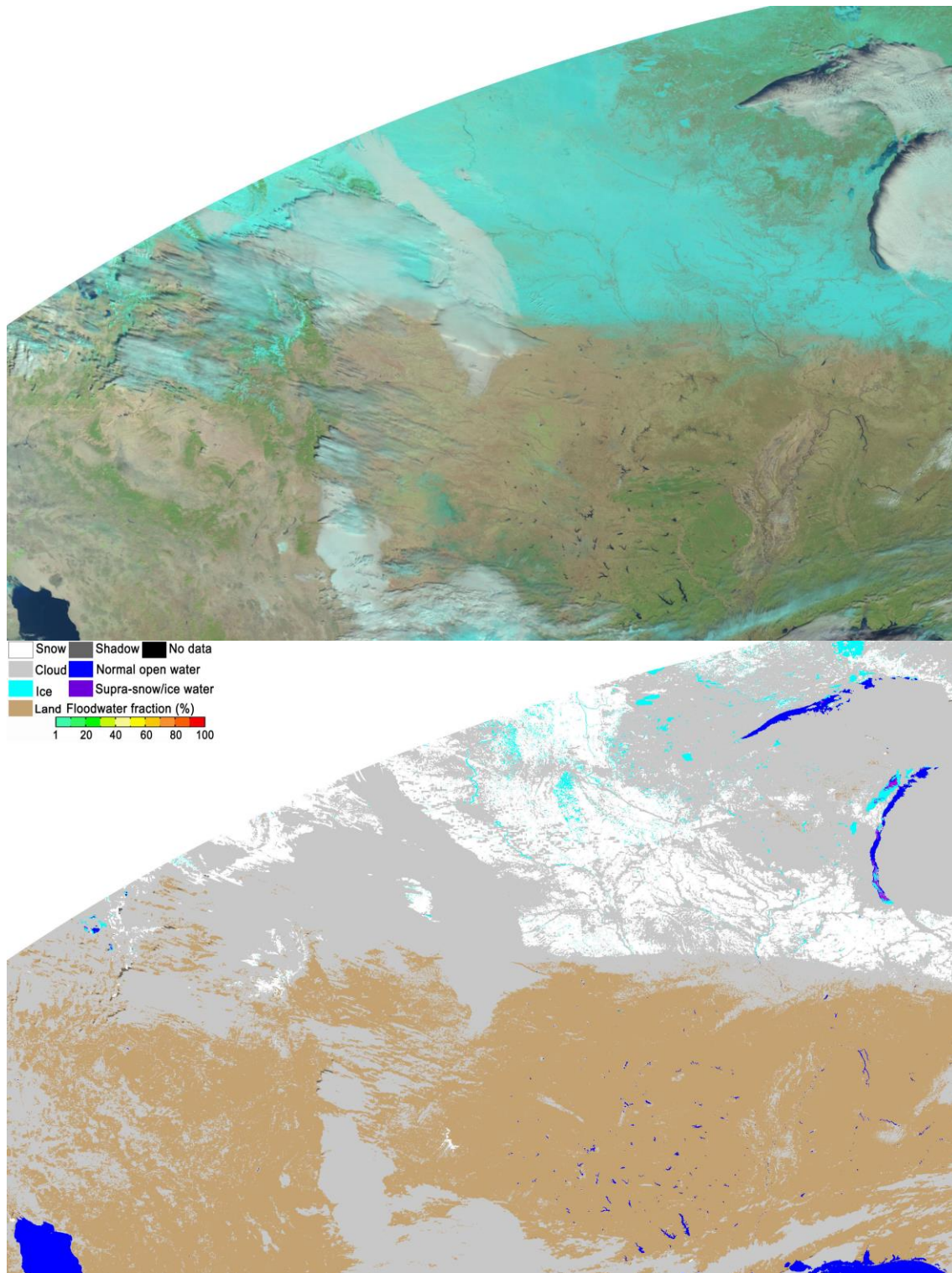


Fig.3 GOES-16/ABI false-color composited image (top) and the corresponding flood map (bottom) on Jan. 01, 2018 16:48 (UTC)

1.2. Correction on the reflectance channels

It is unsure what might cause the diurnal change on the reflectance in the ABI imagery. The most convincing point might be the BRDF or anisotropy of different land types after communicating with the ABI calibration group. However, BRDF correction is a complex process and worth an independent project to solve the problem. After analyzing on the ABI data year around, it is found that the issue is

mainly related to the solar zenith angles and solar azimuth angles. Therefore, a correction method has been developed to decrease the diurnal fluctuation at the ABI reflectance channels.

When solar azimuth angle is less than 180°, the correction reflectance R' is derived using equation (1):

$$R' = R * (1.0 - (0.085 + \sin(0.15 * \theta_n) * |\cos(\delta)|)) * (1.0 + 0.5 * \sin((0.1 - \sin(0.1 * \theta_n) * \theta))) \quad (1)$$

When solar azimuth angle is larger than 180°, the correction reflectance R' is derived using equation (2):

$$R' = R * (1.0 - (0.075 + \sin(0.15 * \theta_n) * |\cos(\delta)|)) * (1.0 + 0.5 * \sin((0.11 - \sin(0.1 * \theta_n) * \theta))) \quad (2)$$

Where, R is cosine corrected reflectance in ABI visible, near infrared and short-wave infrared channels, θ is solar zenith angle, δ is solar azimuth angle, and θ_n is noontime solar zenith angle.

With the Equations (1) and (2), the reflectance in ABI visible, near infrared, and short-wave infrared channels has been corrected. Fig. 4 presents a comparison between the original reflectance (blue series) and the corrected reflectance (red series). From Fig. 4, although the diurnal change pattern still exists, the fluctuation of reflectance has been decreased.

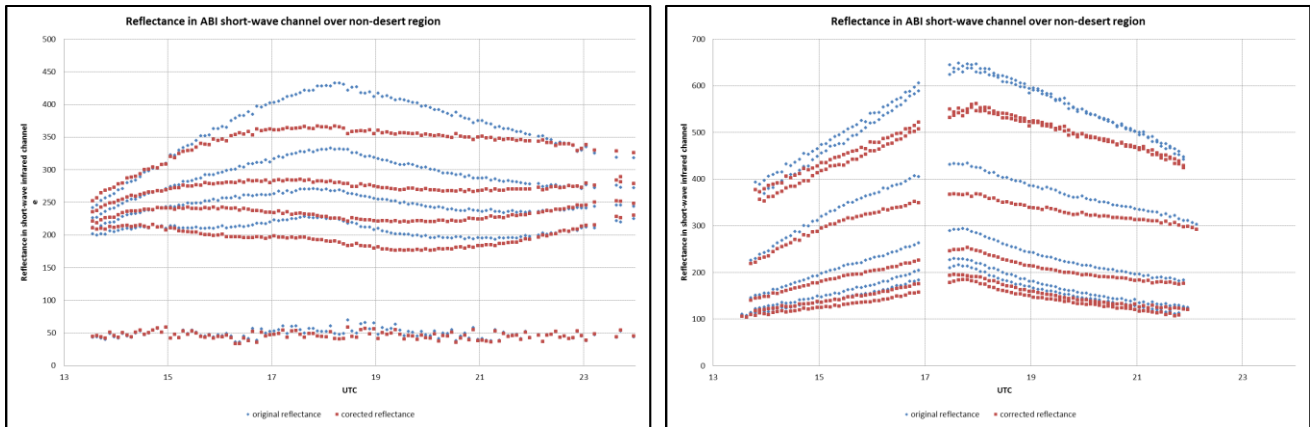


Fig. 4 Comparison between the original reflectance (blue series) and the corrected reflectance (red series) in the ABI short-wave infrared channel

With the corrected reflectance, the flood detection shows more reasonable and consistent results. Fig. 5 presents the corresponding flood map of Fig. 3 using the corrected reflectance. Compared to the flood map in Fig. 3 using the original reflectance, this flood map shows more correct classification results in cloud, snow/ice cover and water detection. With further comparison between the two results, shown in Fig. 6, presents a result that the Lower Mississippi River, which was mostly invisible in the Fig. 6 (left) with the original reflectance, was mostly picked up in the Fig. 6 (right) with the corrected reflectance. In addition, some bare lands, which were mistakenly detected as cloud cover in Fig. 6(left), were classified correctly in Fig. 6 (right).

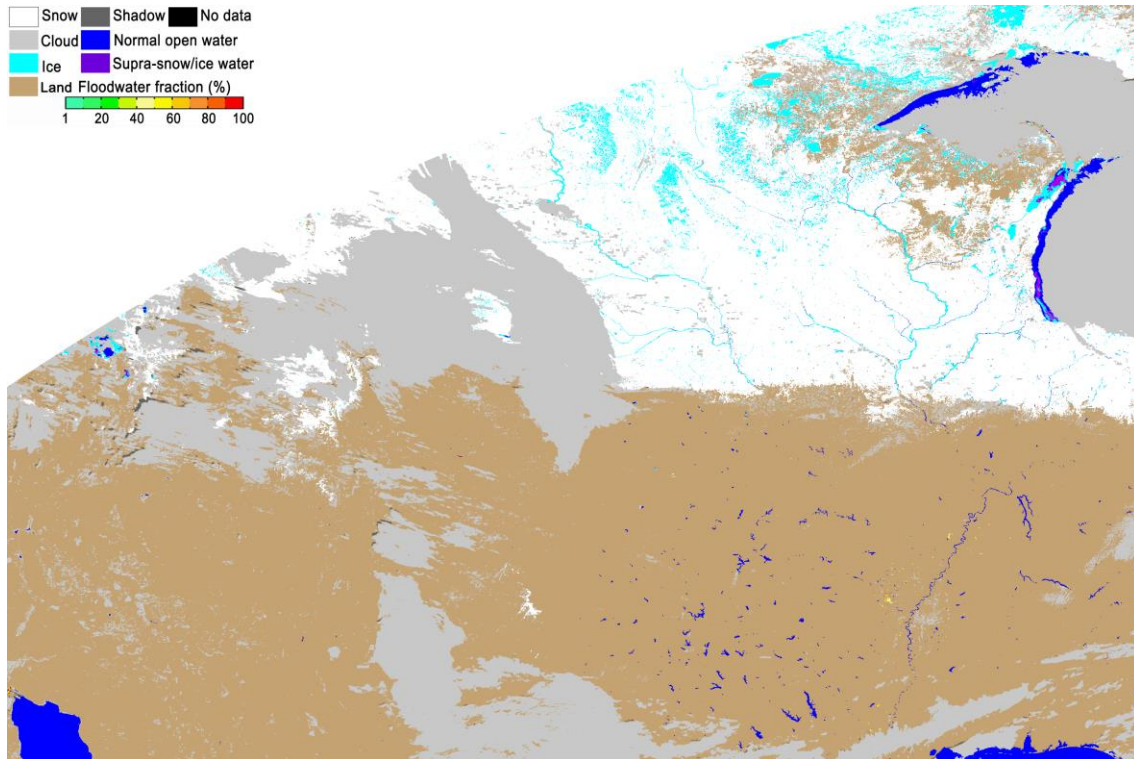


Fig.5 GOES-16/ABI flood map using corrected reflectance (bottom) on Jan. 01, 2018 16:48 (UTC)

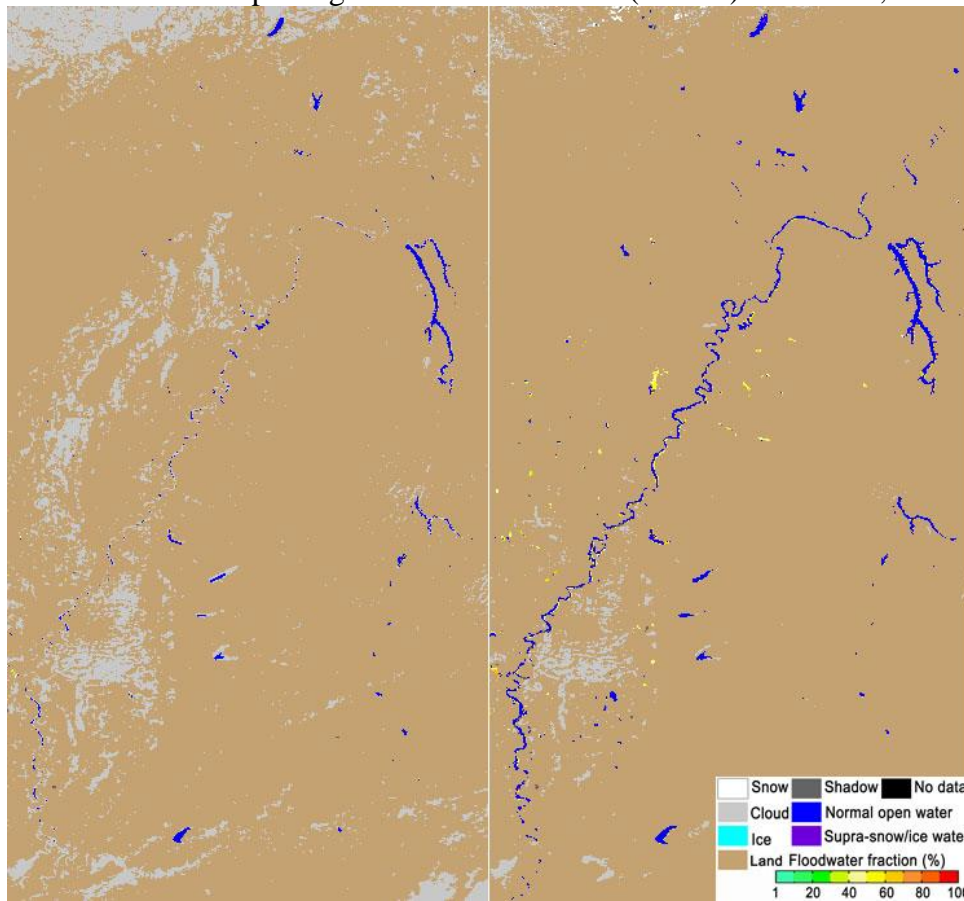


Fig.6 Comparison of GOES-16/ABI flood map using original reflectance (left) and using corrected reflectance (right) on Jan. 01, 2018 16:48 (UTC)

2. Improve the GOES-R flood detection algorithms

2.1. Algorithm improvement

Based on the ABI flood detection algorithms adjusted from VIIRS algorithms, further improvements have been made for better quality. These improvements include:

1) Cloud shadow algorithm improvement: the old cloud shadow algorithm only removes about 90% cloud shadows. To remove the rest cloud shadows, issues in the old algorithm have been fixed including the geometry models over ideal plane and spherical plane, cloud height estimate over thin clouds, and so on. With the new cloud shadow algorithm, more than 95% cloud shadows can be accurately removed.

2) New training on the decision trees: Although the data correction helps decrease the fluctuation of surface reflectance during daytime, the corrected reflectance between 16:00 and 18:00 UTC is still higher than VIIRS imagery. Therefore, new decision trees have been trained over desert and other barren land types to improve the accuracy of classification results.

3) Improvement of the snow/ice detection algorithm: The snow/ice detection algorithm using VIIRS imagery is developed based on single noon-time data. However, the ABI detection is from the early morning to the late afternoon, during which period the diurnal change of the surface temperature must be considered. Therefore, we adjusted the snow/ice detection algorithm by considering the diurnal change of LST. The improved algorithm can detect snow/ice cover in the ABI imagery accurately, which guarantees the quality of water fraction retrieval.

4) Improvement of the water fraction retrieval algorithm: The water fraction retrieval algorithm has also been improved. The improvements are made by more accurate estimate on the reflectance of pure water surface and adjusted thresholds of non-water fractions in the ABI imagery. With the improved algorithm, the water fraction retrieval is more robust.

5) Improvement of the minor water detection algorithm: Due to the different calibration performance, the VIIRS minor water detection algorithm cannot be applied in the ABI imagery directly. Therefore, the algorithm has been adjusted with new thresholds based on the ABI calibration performance.

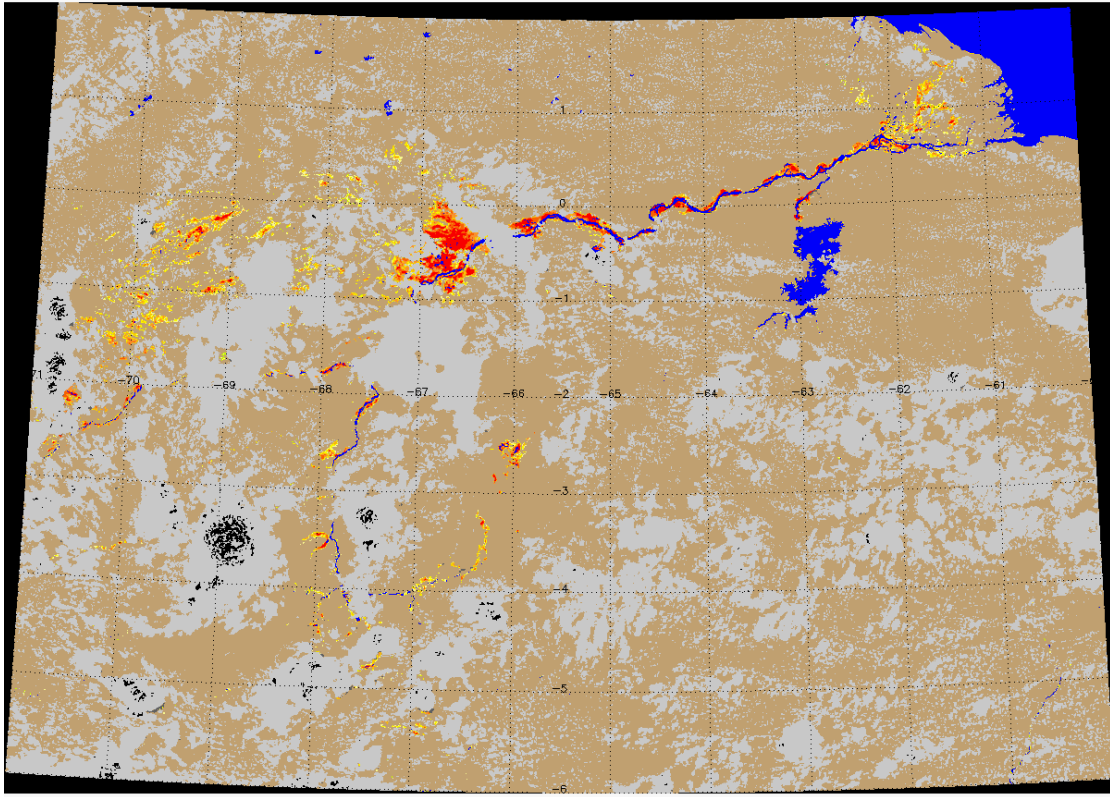
With the above improvements, the ABI flood detection algorithm can be used to generate ABI flood maps with consistent performance.

2.2. Algorithm and software test

The improved ABI flood mapping algorithm and software has been tested with ABI imagery year around. Visual inspection on the ABI false-color images and the corresponding flood maps shows consistent results. The ABI flood detection results are also compared with the corresponding VIIRS results and show consistency with VIIRS. Fig. 7 presents two flood maps from GOES-16/ABI and Suomi-NPP/VIIRS on Aug. 16, 2018. Although the retrieved water fractions are a little bit different due to the difference of spatial resolution and sun-glint contamination, the ABI flood detected results are consistent with the VIIRS results.

Further tests will be performed in the next period till the performance is steady enough for routine process.

ABI Flood Map 20180816 17:21(UTC)



VIIRS Flood Map 20180816 17:30(UTC)

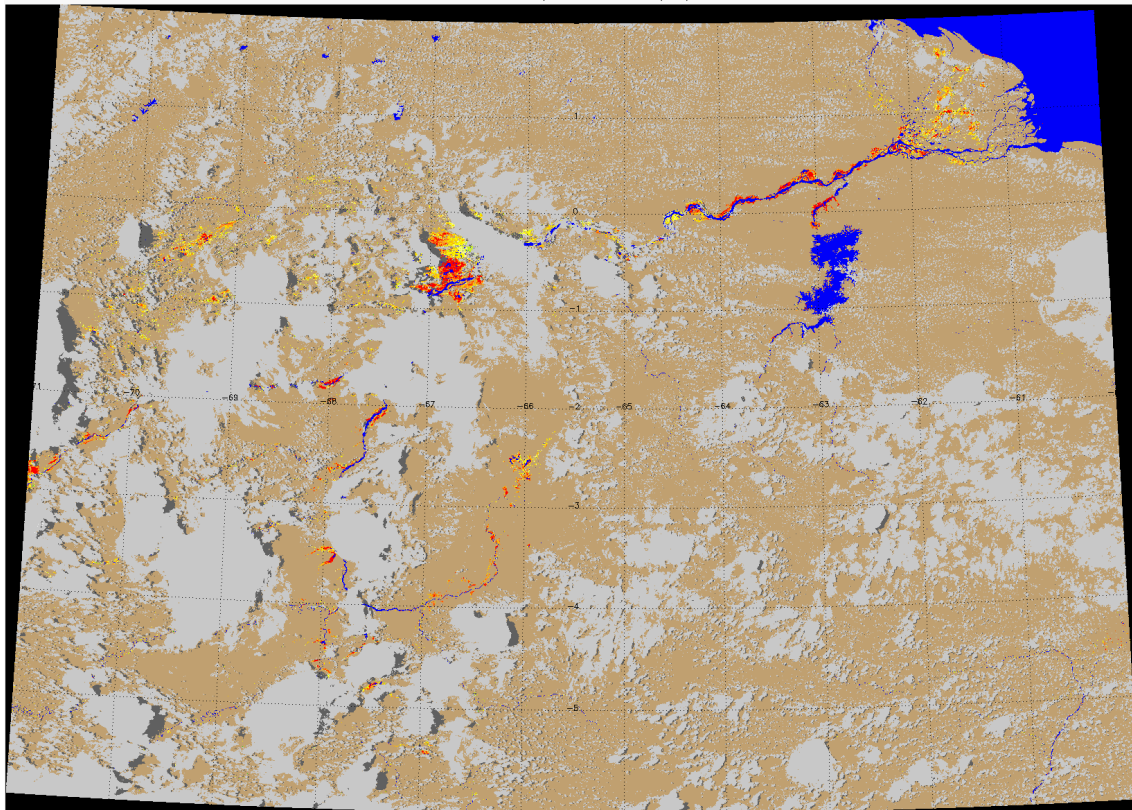


Fig. 7 Flood maps in Venezuela on Aug. 16, 2018 (top: GOES-R/ABI flood map at 17:21 (UTC); bottom: VIIRS flood map at 17:30 (UTC))

3. Near real-time response to flood events with the experimental GOES-R/ABI flood maps

We also applied the ABI imagery in emergency response on the flood events. Fig. 8 shows two ABI composited flood maps in Venezuela on Aug. 11 (top) and Aug. 16 (bottom), respectively, to respond the Venezuela flood activation from International Charter. With the ABI imagery, more clear-sky coverage is derived, which produces clear-sky flood maps in Venezuela from Aug. 11 to Aug. 16 almost every day. This capability helps improve the quality of flood detection substantially.

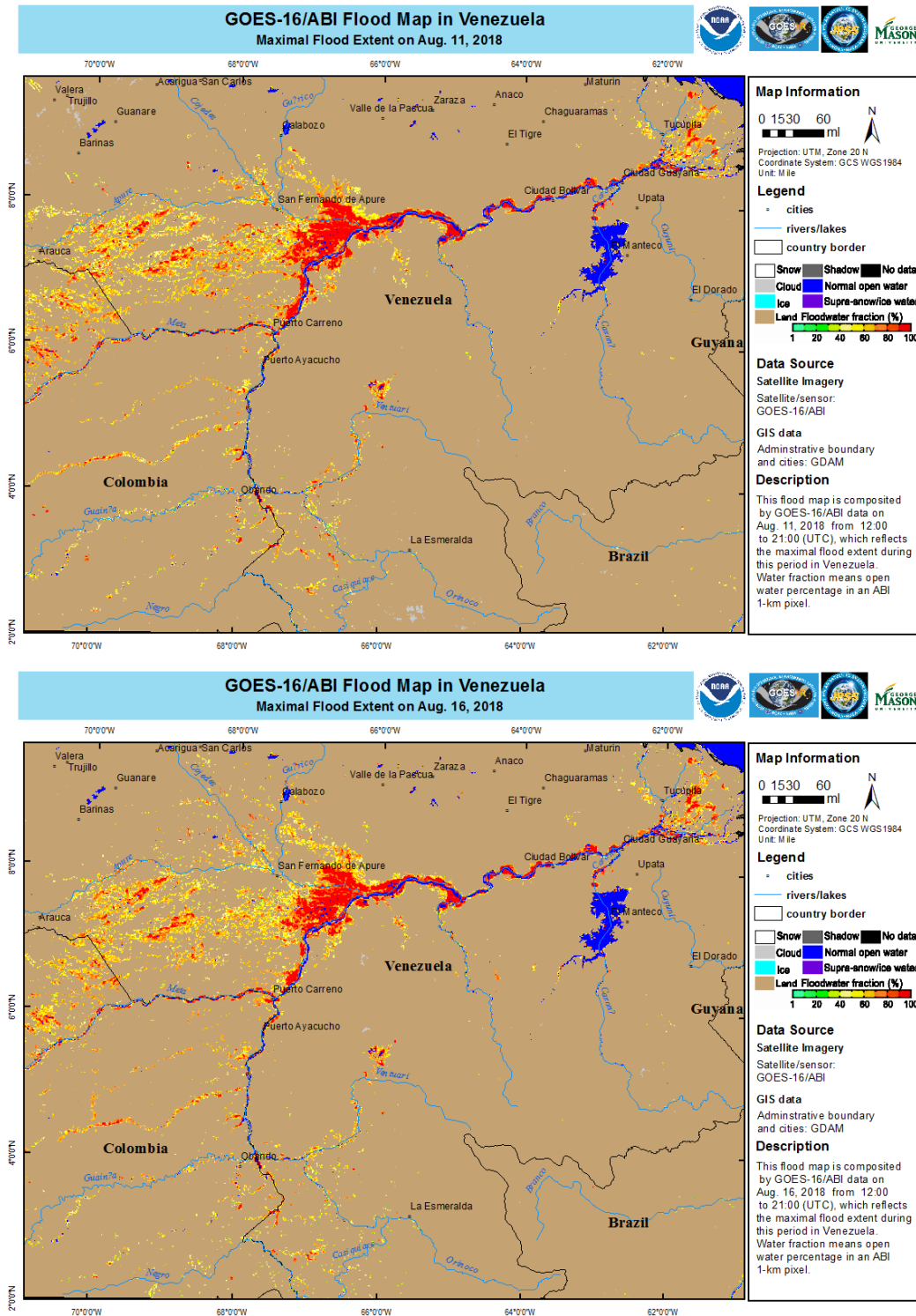


Fig. 8 GOES-R/ABI flood map in Venezuela on Aug. 11 (top) and Aug. 16 (bottom), 2018

4. Issues with the current software

Although the improved algorithms help stabilize the performance of ABI flood mapping, there are still issues with the current algorithms. One major issue is the sun-glint contamination. Severe sun-glint contaminated water surface is generally detected as cloud cover. Water surface with slight sun-glint-contamination can still be detected as water. However, due to the reflectance change of water surface, water fractions are systematically underestimated with the current dynamic nearest neighboring searching method. Further development will be required to either improve the accuracy of both water detection and water fraction retrieval under sun-glint contamination.

The continuity of water detection and water fraction retrieval is still an issue of the current algorithms due to the diurnal change of surface reflectance in the ABI imagery.

Additional Information

1. Interaction with operational partners

We attend monthly telecons organized by the JPSS Program Office, and communicate with NWS's River Forecast Centers on the progress and the issues we meet during the ABI development. We also communicate with the GOES-R Program on the issues existing in the ABI imagery.

2. Conference/workshop participation

None.

3. Outside project publicity

None.

4. Journal articles

- Contributions of Operational Satellites in Monitoring the Catastrophic Floodwaters Due to Hurricane Harvey, Remote Sens. 2018, 10, 1256; doi:10.3390/rs10081256

Plans for the next Reporting Period:

1. Continue to improve the accuracy of the ABI flood detection algorithms.
2. Improve the composition algorithm to reduce the impact of cloud shadows and geolocation errors.
3. Conduct more software tests and further improve algorithm performance.
4. Prepare to deliver the software for the routine process.